Application of optical diffraction method in designing phase plates

Ze-Min Lei(雷泽民)[1,2], Xiao-Yan Sun(孙晓艳)[1,2], Feng-Nian Lv(吕凤年)[1], Zhen Zhang(张臻)[1], and Xing-Qiang Lu(卢兴强)[1,†]

[1] *Key Laboratory on High Power Laser and Physics, Shanghai Institute of Optics and Fine Mechanics, Chinese Academy of Sciences, Shanghai* 201800, *China*

[2] *University of Chinese Academy of Sciences, Beijing* 100049, *China*

(Received 9 May 2016; revised manuscript received 17 June 2016; published online 28 September 2016)

Continuous phase plate (CPP), which has a function of beam shaping in laser systems, is one kind of important diffractive optics. Based on the Fourier transform of the Gerchberg–Saxton (G–S) algorithm for designing CPP, we proposed an optical diffraction method according to the real system conditions. A thin lens can complete the Fourier transform of the input signal and the inverse propagation of light can be implemented in a program. Using both of the two functions can realize the iteration process to calculate the near-field distribution of light and the far-field repeatedly, which is similar to the G–S algorithm. The results show that using the optical diffraction method can design a CPP for a complicated laser system, and make the CPP have abilities of beam shaping and phase compensation for the phase aberration of the system. The method can improve the adaptation of the phase plate in systems with phase aberrations.

Keywords: phase retrieval, diffraction and scattering, optical design and manufacture, continuous phase plate

PACS: 42.30.Rx, 42.25.Fx **DOI:** 10.1088/1674-1056/25/11/114201

1. Introduction

In high power laser facilities, the uniformity of laser irradiation on the target has extremely strict requirements.[1] In order to meet such requirements, various laser beam smoothing techniques have been put forward, including two-dimensional smoothing by spectral dispersion (SSD),[2,3] polarization smoothing (PS),[4,5] segmented wedge array (SWA),[6] distributed phase plates (DPP),[7,8] and continuous phase plates (CPP).[9–11] All of these measures have their unique performances. Among them, CPP has been widely used because of its great control of the far-field pattern and smoothing effects.[11–13] CPP is a kind of important diffractive optics with complex figure. The design of CPP is similar to the other diffractive optical elements, mainly involving a phase retrieval process, and there are various design algorithms, including the Gerchberg–Saxton (G–S) algorithm, simulated annealing,[14,15] the genetic algorithm,[16] and some modified algorithms based on these standard ones.[17] The G–S algorithm, which can design CPP to meet the demand of experiments, has advantages of fast calculation speed and convenient implementation, resulting in wide applications. The basis of the G–S algorithm is the Fourier transform and its inverse with a many-times iteration process.[18]

The G–S algorithm based on Fourier transform usually calculates under the ideal conditions. The obtained CPP will have a good performance in the system with good beam quality or little phase aberration. But when the beam quality is not so good or the system has large total phase aberrations, the performance of the CPP will be affected.[11,12] If these factors of the system can be taken into account in the design, the result of the new CPP will be better than the former one.

In this paper, we firstly introduce the basic principle of the G–S algorithm, then propose our optical diffraction method based on real system conditions. The method is completed by replacing the Fourier transform of G–S with beam propagating through a lens and replacing the inverse Fourier transform with the inverse diffraction from the far-field domain to the near-field domain. The method allows an additional phase modulation to cut in the beam path, especially the space behind the lens. Secondly, a simple and clear example in which this diffraction method is used to design a CPP for a system with a phase modulation is presented. Besides, a comparison of the CPP shaping results obtained by the two different design methods is performed. Lastly, for a simplified and scaled system from the final part of a real laser facility,[19] the steps of designing a CPP using the proposed method are described.

2. Principles of the two CPP design methods

2.1. Standard G–S algorithm

The G–S algorithm is a type of iterative optimization algorithm based on the Fourier transform.[20] A diagram of the iterative procedure with some important parameters is presented in Fig. 1. Five steps of the process are described as follows. 1) φ_{DPP} is the initial phase generated randomly, E_0 is the objective near-field amplitude, and they can form a complex field of the input beam. 2) E_{f} is the complex amplitude in the far-field made by the spatial Fourier transform of the near-field. 3) Judge if the E_{f} is an appropriate output result. 4) If E_{f}

†Corresponding author. E-mail: xingqianglu@siom.ac.cn

© 2016 Chinese Physical Society and IOP Publishing Ltd

is not suitable, the far-field objective pattern E_{obj} replaces the calculated amplitude of the far-field, and the far-field phase distribution generated by step 2) and E_{obj} form a new far-field distribution. 5) Make an inverse Fourier transform of the new far-field obtained in step 4), and obtain a new near-field distribution. The phase information φ_{DPP} is the required key output result, and it also goes into step 1) to become the phase distribution in the next iterative process. Then do the process again until the result φ_{DPP} is appropriate.

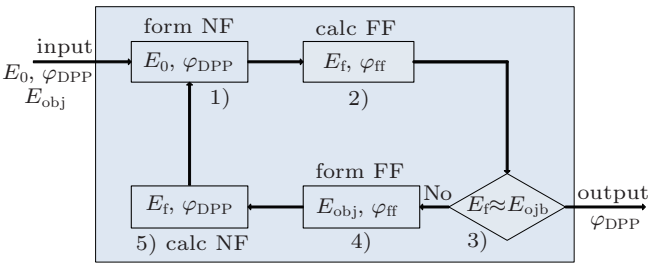


Fig. 1. Standard G–S algorithm flow diagram.

2.2. Principle of the optical diffraction method

According to the G–S algorithm principle described in Subsection 2.1, the Fourier transform is the basis of the algorithm.[21–23] Based on Fourier optics knowledge, a thin lens can complete the Fourier transform of the input signal and gain the result on the focal plane. The inverse Fourier transform just corresponds to the inverse process of the focusing function of a thin lens, which means light propagates back to the near-field domain from the far-field domain. This inverse propagation process can be run on a program. Figure 2 is the schematic of the proposed optical diffraction method. Figure 2(a) shows the focusing process of a lens corresponding to the Fourier transform, and figure 2(b) shows the inverse process. The dashed dot lines in Fig. 2(b) are to distinguish the inverse process of light from the normal propagation. The iteration step and analysis of the method are given below.

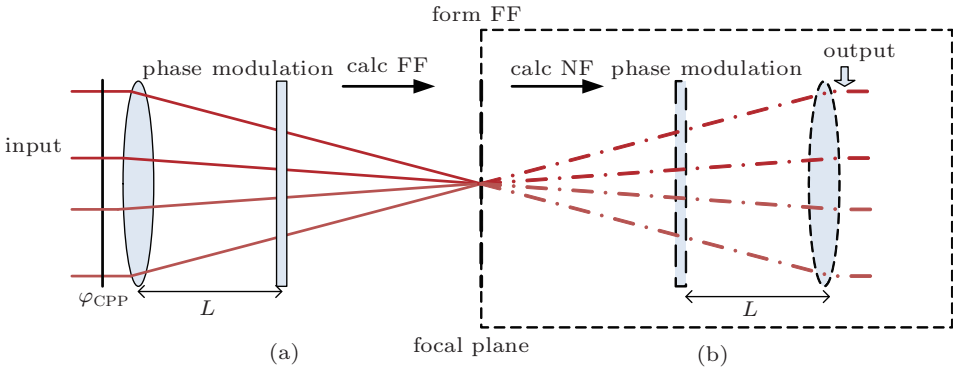


Fig. 2. (color online) Diagram of the optical diffraction method: (a) the focusing process of a lens corresponding to the Fourier transform, (b) the inverse process.

The diffraction method aiming to design CPP is tantamount to calculating the propagation and the inverse propagation of light in Fig. 2. The light propagation can be described by the scalar diffraction theory. The input laser is assumed to be a flat-top beam and its complex amplitude is U_1. φ_{CPP} is the modulation caused by a phase plate and also is the result we demanded. At first, a random phase distribution is set as φ_{CPP}, which will change during each iteration process. The function of the thin lens is known as

$$t_l = \exp\left[-\mathrm{j}\frac{k}{2f}\left(x^2+y^2\right)\right]. \tag{1}$$

The beam propagates a certain distance L after passing the lens to meet a kind of phase modulation φ. Then the beam further propagates a distance $(f-L)$ to go to the focal plane. Figure 2(a) shows the focusing process which can be expressed as

$$U_f = U_1 \exp(\mathrm{j}\varphi_{CPP}) t_l \otimes h_{z=L} \exp(\mathrm{j}\varphi) \otimes h_{z=f-L}, \tag{2}$$

where U_f is the far-field complex amplitude, $\otimes$ donates the convolution, and h is the pulse response function of diffractive propagation under the Fresnel approximate conditions. The h is a function of propagation distance z

$$h_z(x,y) = \frac{\exp(\mathrm{j}kz)}{\mathrm{j}\lambda z} \exp\left[\mathrm{j}\frac{k}{2z}\left(x^2+y^2\right)\right], \tag{3}$$

where $k = 2\pi/\lambda$ and λ is the wavelength.

When far-field distribution U_f on the focal plane is obtained, the phase part of U_f and the objective amplitude combine to form a new far-field complex just like that in the G–S algorithm mentioned above. The new distribution is expressed as

$$U_f' = E_{obj} \exp(\mathrm{j}\varphi_{ff}), \tag{4}$$

where φ_{ff} is the phase part of U_f calculated by Eq. (2), and E_{obj} is the objective amplitude and usually a round super-Gaussian distribution for the focal spot.

Figure 2(b) shows the inverse process. The new far-field U_f' is the input signal and the inverse propagating process can be expressed as

$$U_1' = U_f' \otimes h_{z=f-L}^{-1} \exp(-\mathrm{j}\varphi) \otimes h_{z=L}^{-1} t_l^{-1}, \tag{5}$$

where h^{-1} is the pulse response function of inverse diffractive propagation and just a small change is added to Eq. (3),

$$h_z^{-1}(x,y) = \frac{\exp(-\mathrm{j}kz)}{-\mathrm{j}\lambda z}\exp\left[-\mathrm{j}\frac{k}{2z}\left(x^2+y^2\right)\right]. \tag{6}$$

The change of function t_l^{-1} is the same as that of h^{-1}. It means that the phase factor introduced by the lens is eliminated from the phase information of the beam. t_l^{-1} is expressed as

$$t_l^{-1} = \exp\left[-\mathrm{j}\frac{k}{-2f}\left(x^2+y^2\right)\right]. \tag{7}$$

The result we needed is the phase part of the output beam according to $U_1' = U_1\exp(\mathrm{j}\varphi_{\mathrm{CPP}})$, which is obtained by a comparison of Eqs. (2) and (5). This is a complete calculation process and lots of calculation time is needed to obtain an optimized result. U_1' must be handled just like U_f before it can go into the next iteration process. The phase part of U_1' and the objective near-field amplitude combine to form the new input beam that goes into the calculation process.

The whole optical diffraction method is based on the beam diffractive propagation implemented by numerical simulation. According to Fig. 2, the biggest difference between the diffraction method and the G–S algorithm is the phase modulation φ located in the space behind the lens. The phase modulation is considered in our design. φ in Eq. (2) can express a single phase modulation or multi-modulations

$$\begin{aligned}\exp(\mathrm{j}\varphi) &= \exp(\mathrm{j}\varphi_1)\otimes h_{z_1}\cdot\exp(\mathrm{j}\varphi_2)\\ &\quad\otimes h_{z_2}\cdots h_{z_{n-1}}\cdot\exp(\mathrm{j}\varphi_n),\end{aligned} \tag{8}$$

or some modulation like atmosphere disturbance

$$\exp(\mathrm{j}\varphi) = \exp[\mathrm{j}\varphi(z,t)]. \tag{9}$$

2.3. Quality evaluation of the focal spot

Two specifications, root mean square (RMS) and energy concentration η, of the focal spot are used to measure the shaping ability of CPP. They are defined as

$$N_{\mathrm{RMS}} = \sqrt{\frac{\sum\limits_{S_{\mathrm{top}}}\left|I-\bar{I}\right|^2/\bar{I}^2}{N-1}}, \tag{10}$$

$$\eta = \frac{\sum\limits_{S_{\mathrm{top}}} I}{\sum\limits_{S_{\mathrm{total}}} I}, \tag{11}$$

where I is the intensity of the sampling points, $\bar{I}$ is the average intensity of I, N is the number of the sampling points, and S_{top} and S_{total} are the area of the objective far-field and the area of the total spot, respectively.

3. CPP designed by the optical diffraction method

Figure 2 shows the schematic of the optical diffraction method to design a CPP based on the real optical path. So figure 2(a) is also a simple optical system which needs a CPP to shape the laser beam. The phase modulation is set as a cosinoidal type presented in Fig. 3, with 5λ peak-to-valley (PV). This value is proper to evaluate the effects of the cosinoidal modulation on the beam quality and the result of CPP. The objective far-field intensity envelope is a super-Gaussian of order 4 with an intensity full width at half-maximum (IFWHM) radius of $r = 0.4$ mm. The near-field clear aperture is square with a side length of 40 mm. The focal length is 1800 mm and the wavelength is 351 nm. The simulation space for the near field is a 2048×2048 grid. The distance L between the lens and the position of modulation is 1000 mm. The whole calculation process needs 20 iterations without filter plus 50 iterations with a super-Gaussian filter of order 20 and filter cutoff parameter 317 rad/m.[24]

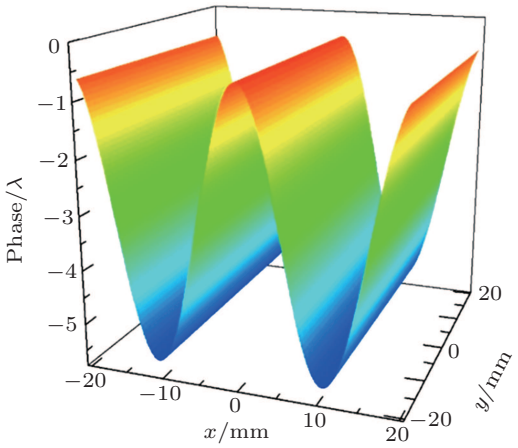


Fig. 3. (color online) Three-dimensional distribution of cosinoidal phase modulation.

The periodic phase modulation shown in Fig. 3 has a very significant influence on the beam quality due to its grating-like function of spectral dispersion. Especially when the modulation depth is relatively large (several wavelengths), lots of beam energy will be transferred to the sidelobes of the focal spot. Therefore, this type of modulation introduced into the system can affect the performance of the shaping optics seriously, CPP in this case. This cosinoidal phase modulation is taken into account in the optical diffraction method and the results are shown in Fig. 4. Figure 4(a) is the continuous phase plate calculated by the diffraction method. According to the figure, it has a low distribution on the center and high distributions on both sides. This feature of the distribution is opposite to the cosinoidal distribution in Fig. 3. Figure 4(b) plots the lines of distributions of the CPP along x and y axes. The line along the x axis has a large valley distribution with about 5λ

of PV, while the line along the y axis does not have such a large PV. Note that only the center portion of the phase modulation is valid because the beam size becomes smaller after propagating a distance behind the lens.

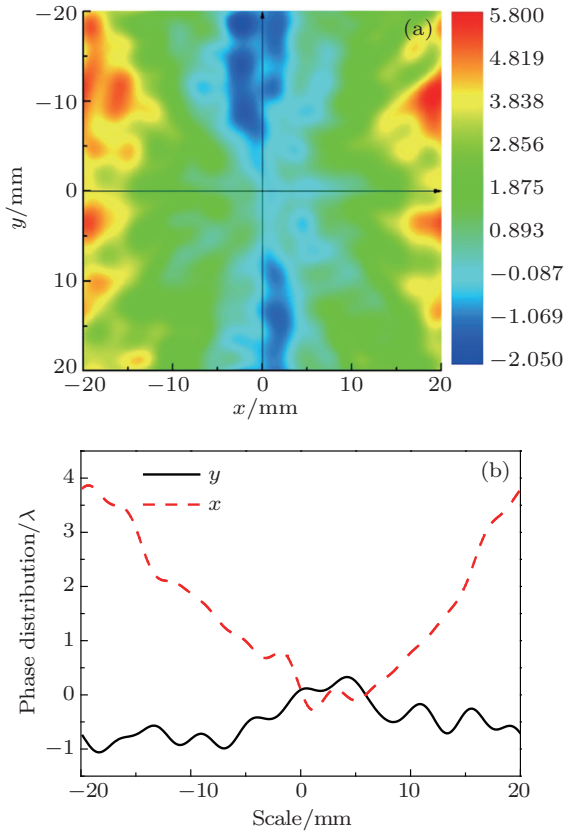


Fig. 4. (color online) (a) Continuous phase plate calculated by the diffraction method; (b) one-dimensional distributions of CPP along x and y axes.

As a contrast, another CPP is designed by the traditional G–S algorithm. The result is presented in Fig. 5. Figure 5 is the figure distribution of the phase plate and has no discernible distribution features (the radiating-like shape is just caused by the phase unwrapping algorithm). Figure 5(b) shows the lines of the CPP distribution along x and y axes and the PV of this CPP is just about 1λ.

Both CPPs calculated above are applied to the system and their shaping results of the focal spot are presented in Fig. 6. It is clear that the spot in Fig. 6(a) shaped by the CPP in Fig. 4 is better than that in Fig. 6(b) shaped by the CPP in Fig. 5. The RMS value of the top area and the energy concentration are 13.2% and 85.5% for the spot in Fig. 6(a), and 17.0% and 76.9% for the spot in Fig. 6(b). This difference is caused by the cosinoidal phase modulation, which is considered in the diffraction method but not in the G–S algorithm. This difference is related to the PV of the modulation. So it indicates that the CPP designed by G–S can have a good performance when the phase aberrations in an optical system are small. But when the phase aberrations become larger, the diffraction method will have more advantages.

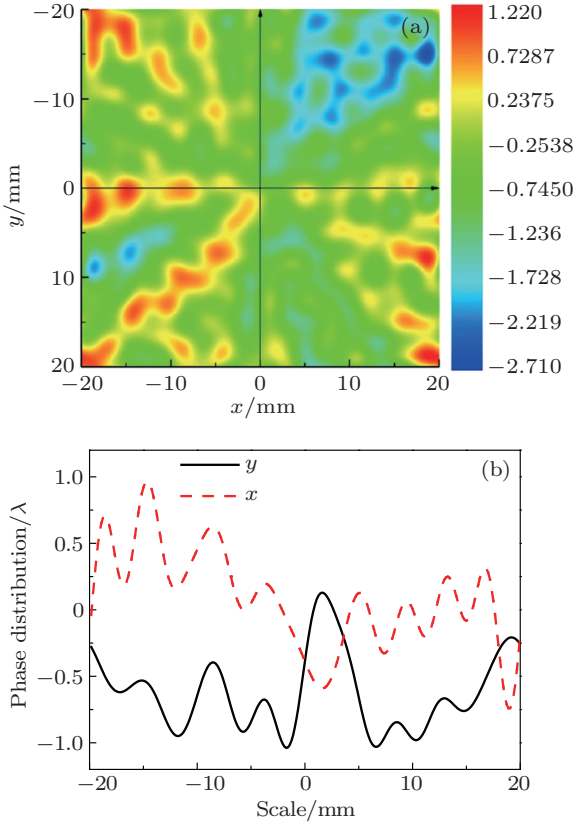


Fig. 5. (color online) (a) Continuous phase plate calculated by the G–S algorithm; (b) one-dimensional distributions of CPP along x and y axes.

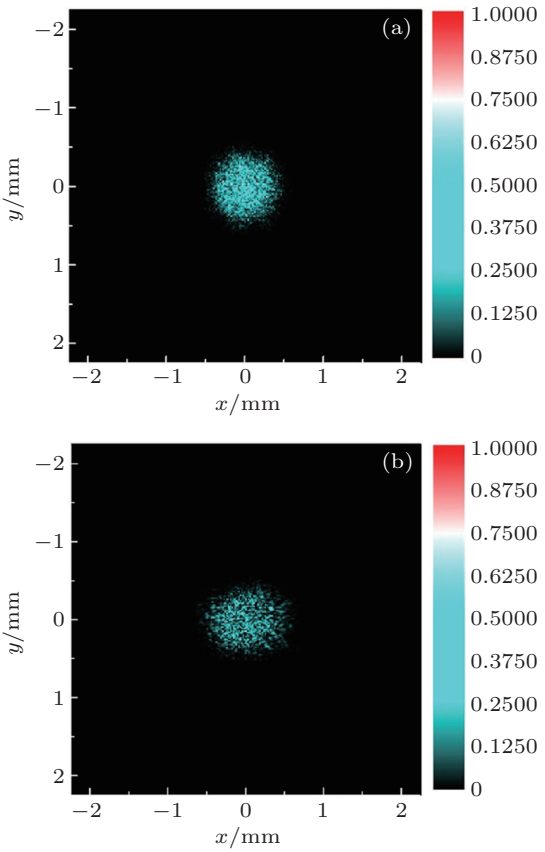


Fig. 6. (color online) Two-dimensional distributions of focal spots: (a) shaped by the CPP in Fig. 4, (b) shaped by the CPP in Fig. 5.

4. Application of the diffraction method in a system

A typical final optics assembly of a high power laser facility is shown in Fig. 7. The schematic has been simplified on the basis of a real system as follows: 1) a normal thin lens replaces the wedged lens that has another function of spectral dispersion; 2) there are three frequencies of light in the final part of the laser system, and only one wavelength is presented for design. All these simplifications are appropriate to emphasize the effects of the layout and quality of optics. The input beam shown in Fig. 7 is not ideal as it comes from the upstream chain of the laser system. The beam is modulated by the window component when passing through it. The light continues to go through CPP, lens, two other optics behind the lens, and finally arrives at the target. These components can definitely cause aberrations of the beam and affect the quality of the far-field spot. Here are the procedures of using the optical diffraction method to design CPP for this system.

The parameters of this system are nearly the same as those in Section 3, except for the phase modulations caused by real optics. Based on the principle of the design method, this system will be separated into two parts: part one is for the optical path after the lens (including the lens) and similar to the system in Section 3; part two is for the window and the input beam with phase distortion.

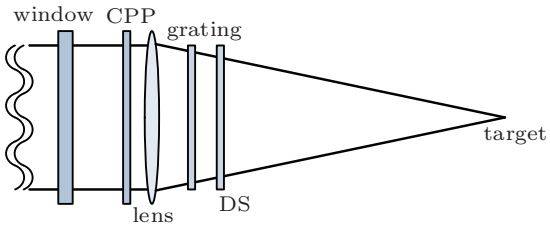


Fig. 7. Simplified schematic of the final part of a high power laser facility.

4.1. Step 1 for part one

This step for part one is to calculate the near-field phase distribution just before the lens. The calculating process is shown in Fig. 8, just another phase modulation added in the optical path compared to Fig. 2. Two of the phase modulations are marked as PM 1 and PM 2 in the figure. The distances L_1 between the lens and PM 1 and L_2 between PM 1 and PM 2 are 300 mm and 100 mm, respectively. PM 1 and PM 2 are transmitted wavefronts coming from measurements on the real optics, as shown in Fig. 9. These two optics have a flat surface figure in general, with some small defects of the fringes.

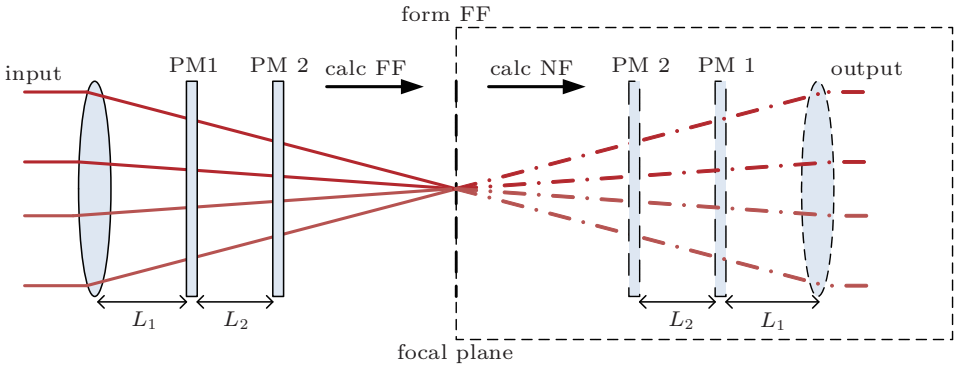


Fig. 8. (color online) Schematic of the diffraction method with two modulations to calculate the phase distribution.

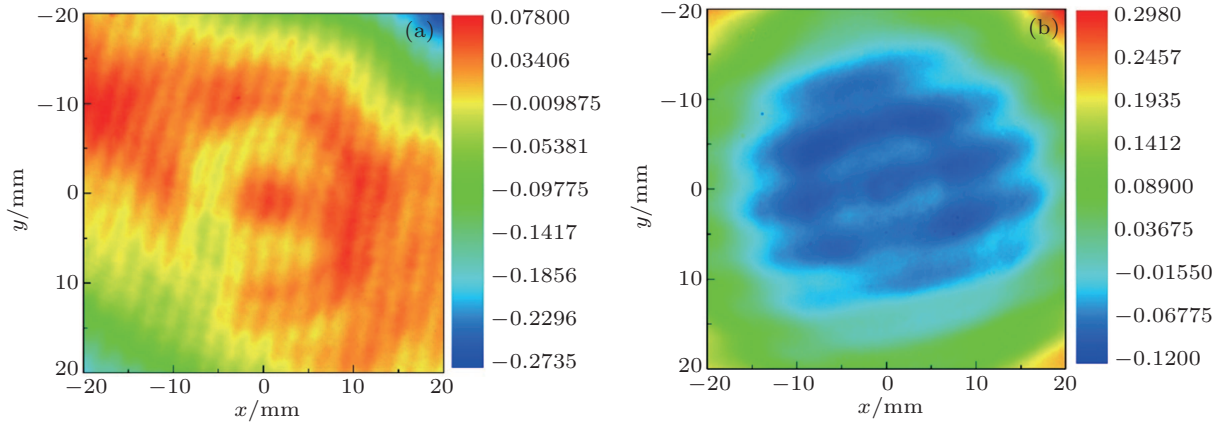


Fig. 9. (color online) (a) Wavefront distribution of PM 1; (b) wavefront distribution of PM 2.

This part of the calculation is for the near-field phase information just before the lens, which is also the result of CPP in the case of Section 3. But in the system of Fig. 7, there are other conditions to consider. The result of the phase distribution obtained in this step is denoted as near-field phase 1, just for the next step to calculate.

4.2. Step 2 for part two

Part two is to calculate the effects of the window component and the distorted input beam. Two phase modulations are denoted by PM 3 and PM 4, as presented in Fig. 10. This step is to conduct a simple operation on near-field phase 1, as illustrated in Fig. 11. The section surrounded by huge brackets is the phase distribution which contains effects of the input beam distortion PM 3, modulation caused by window PM 4, and diffractive propagation in free space. The result of CPP is the difference between these two phase distributions. The length of free space or the distance between the window and the CPP in the system is 1000 mm.

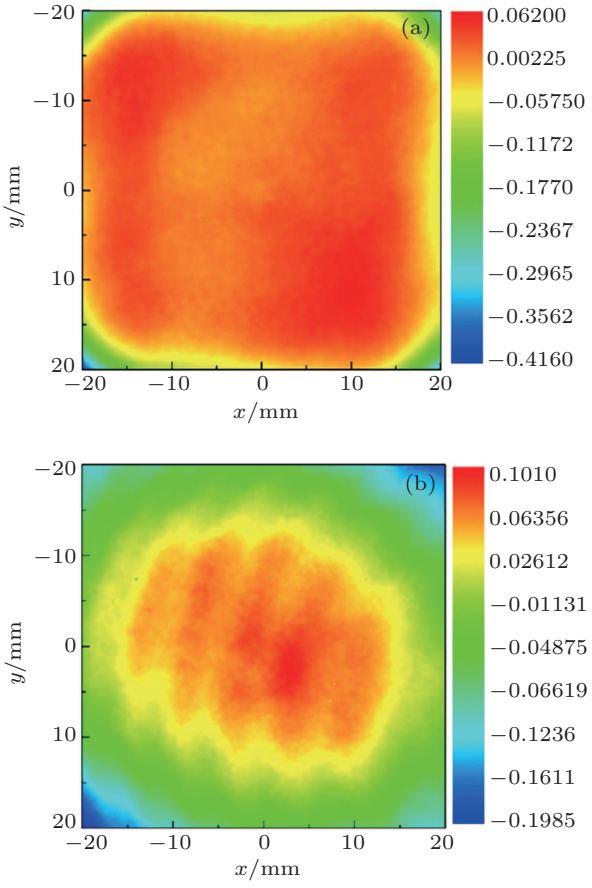


Fig. 10. (color online) (a) PM 3: phase distortion of the input beam; (b) PM 4: wavefront distribution of the window.

The final result of CPP is shown in Fig. 12(a) and the focal spot shaped by CPP is shown in Fig. 12(b). The RMS value of the top area and the energy concentration of the focal spot in Fig. 12(b) are 12.9% and 85.2%, respectively, which explains the good performance of the designed CPP.

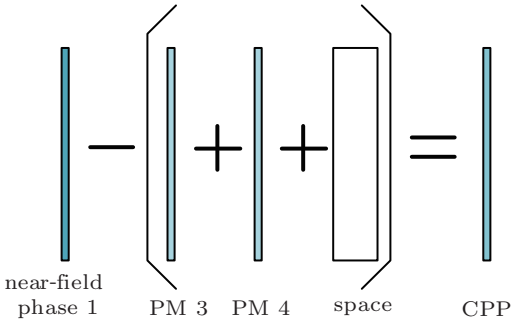


Fig. 11. (color online) Calculation of the near-field phase distributions.

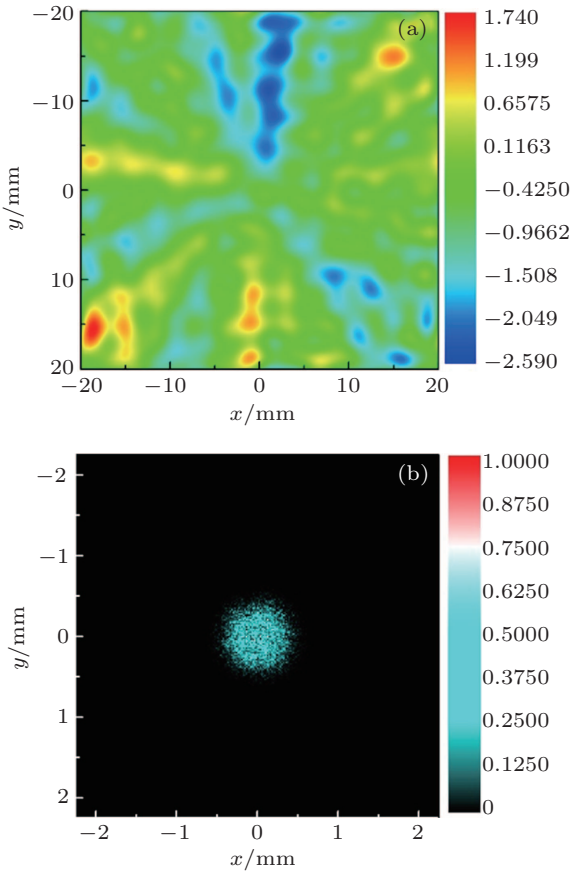


Fig. 12. (color online) (a) Distribution of the calculated CPP; (b) the focal spot shaped by the CPP.

5. Conclusion

An optical diffraction method is proposed to design CPP based on the standard G–S algorithm. The transformation of near-field and far-field of light is completed by Fresnel diffractive propagation and inverse propagation. Multiple iterations are also necessary to optimize the phase result just as in the G–S method. The difference between them is that the diffraction method can take diffraction effects of propagation and the layout of optics in the system into consideration. The results in Section 3 show the feature and the validity of the diffraction method by designing a CPP for a system with a cosinoidal phase modulation. Then good shaping performance is obtained by using the diffraction method in a more compli-

cated system. The continuous phase plate designed by this method can improve the influence of the phase modulation on the shaping performance, especially when these modulations are in the position after the lens. The method helps to get a more flexible phase plate and improves uniformity of the laser irradiation on the target. The method is not only for designing CPP for beam shaping, but also for other situations that require a phase retrieval algorithm.

References

[1] Stephen E B, Denis G C, John H G, Robert H L, Stephen P O, Lee P, Andrew J S, John D S, Robert L M C, Wolf S, Charles P V, James P K, Bedros B A and Howard T P 1998 *Phys. Plamas* **5** 1901

[2] Sean P R, John A M, Stephen R C, John H K, William R D, Paul A J, Douglas J P, Robert L K, Terrance J K, David D M, Sangster T C, Wolf S, Vladimir A S, Stanley S and Jonathan D Z 2005 *J. Opt. Soc. Am. B* **22** 998

[3] Epstein R 1997 *J. Appl. Phys.* **82** 2123

[4] Boehly T R, Smalyuk V A, Meyerhofer D D, Knauer J P, Bradley D K, Craxton R S, Guardalben M J, Skupsky S and Kessler T J 1999 *J. Appl. Phys.* **85** 3444

[5] Rothenberg J E 2000 *J. Appl. Phys.* **87** 3654

[6] Cai B W, Liu Z Y, Lv B D and Ye Y D 1996 *Chin. J. Lasers* **23** 57 (in Chinese)

[7] Lin Y, Kessler T J and Lawrence G N 1995 *Opt. Lett.* **20** 764

[8] Terrance J K, Ying L, Armstrong J J and Belimar V 1993 *Laser Coherence Control: Technology and Applications Proc. SPIE 1870*, January 17, 1993, Los Angeles, CA, p. 95

[9] Dixit S N, Feit M D, Perry M D and Powell H T 1996 *Opt. Lett.* **21** 1715

[10] Lin Y, Kessler T J and Lawrence G N 1996 *Opt. Lett.* **21** 1703

[11] Marozas J A 2007 *J. Opt. Soc. Am. A* **24** 74

[12] Zhang Y H, Yang C L, Wen S L, Yan H, Wang J and Yang L M 2012 *High Power Laser and Particle Beams* **24** 1741 (in Chinese)

[13] Joshua E R 1997 *J. Opt. Soc. Am. B* **14** 1664

[14] Yang G G 1993 *Acta Optica Sinica* **13** 577 (in Chinese)

[15] Kirpatrick S, Gelatt C D and Vecchi Jr M P 1983 *Science* **220** 671

[16] Mahlab U, Shamir J and Caulfield H J 1991 *Opt. Lett.* **16** 648

[17] Wen S L, Yang C L, Zhou L S and Xu Q 2009 *Laser Technology* **33** 91 (in Chinese)

[18] Wyrowski F and Bryngdahl O 1988 *J. Opt. Soc. Am. A* **5** 1058

[19] Paul J W, Jerome M A, Thomas A B Jr, Sham N D, Janice K L, Joseph A M, Thomas G P, David W S, Pamela K W and Wade H W 2004 *Optical Engineering at the Lawrence Livermore National Laboratory II: The National Ignition Facility*, January 25, 2004, San Jose, CA, p. 5341

[20] Wen S L, Xu Q, Ma P, Yang C L, Zhou L S and Yan H 2009 *Acta Optica Sinica* **29** 3179 (in Chinese)

[21] Goodman J W 1988 *Introduction to Fourier Optics* (New York: McGrawHill)

[22] Born M and Wolf E 1999 *Principles of Optics: Electromagnetic Theory of Propagation, Interference and Diffraction of Light* (Boston: Cambridge University Press)

[23] Fienup J R 1982 *Appl. Opt.* **21** 2758

[24] Lin Z X, Zhang R Z, Yang C L and Xu Q 2010 *High Power Laser and Particle Beams* **22** 2634 (in Chinese)